

Coordination Between Distributed Generation Stability and Undervoltage Protection Requirements at DG Interconnection Point

Ioanna Xyngi, Marjan Popov

Abstract--This paper describes the transient stability analysis of a 10 kV distribution network with wind generators, microturbines and CHP plants. The network being modeled in Matlab/Simulink takes into account detailed dynamic models of the generators. Fault simulations at various locations are investigated. For the studied cases, the critical clearing times are calculated. Some network parameters which influence transient stability are also observed. The ride-through capability of the DG units is studied through transient stability analysis and the equivalent CCT-voltage dip curves are derived. It is concluded that during fault, DG unit availability can be increased through modification of undervoltage protection requirements.

Keywords: critical clearing time, distribution network, distributed generation, fault ride-through.

I. INTRODUCTION

Nowadays, ‘Distributed Generation’ (DG) is gaining much more attention worldwide than ever as an alternative to large scale centralized generating stations. Over the last few years, a number of policy drivers such as economical (energy efficiency), environmental (reduction of gaseous emissions), political (competition) and technical (voltage support) have encouraged this increased interest in distributed generation schemes. The presence of the DG obviously impacts the power system operation. Therefore, the installation of DG sources raises new challenges and various studies have shown the negative DG impact on the host distribution networks.

This paper reports an investigation related to the determination of the Critical Clearing Time (CCT) of DGs when a variety of disturbances occurred on the network. In IEEE report [1] the Critical Clearing Time (CCT) is defined as “the maximum time between the fault initiation and its clearing such that the power system is transiently stable”. For Synchronous Generators (SG) there exists a maximum rotor angle below which SG can retain a stable operation. This position is known as critical clearing angle. The

corresponding maximum clearing time is known as critical clearing time. Unlike SGs, stability of an induction generator can be evaluated based on its mechanical speed [2]. Therefore, the CCT for an induction generator is the maximum time of the fault to be cleared, within a time span that the induction generator is able to retain its stability. Such time will thereafter be referred to as the CCT for induction generator. In this work, the CCT of the distribution network is defined as the smallest from all CCT values for the different generators for each specific fault location.

The study is conducted on a simulated system that consists of a distribution network (DN) with DGs using SimPowerSystems toolbox. Initially, iterative simulations are performed for various three phase faults at different locations. For each fault location, fault duration is iteratively modified until the determination of CCTs. Then, calculation of CCTs is also provided for the DG elements both for external faults and for faults at their terminals. The derived CCT - voltage dip curves reflect the fault ride-through capabilities of the DG units. The comparison of the extracted curves with typical used undervoltage protection requirements reveals meaningful observations. The adjustment of the DG undervoltage protection settings according to the derived curves increases the during-fault DG availability. Finally, results obtained from several case studies are presented and evaluated.

II. MODELING OF THE MV GRID USING MATLAB/SIMULINK

The one-line schematic diagram of the system analyzed in this investigation is shown in Fig 1. Modeling and simulations have been performed by using Matlab/Simulink and SimPowerSystems toolbox. Table 1 describes the type and the number of DGs.

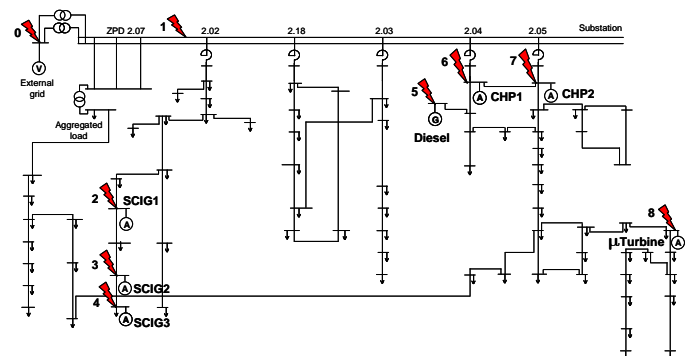


Fig. 1. Schematic diagram of the investigated network with distributed generators.

This work was supported by Senter Novem under grant EMVT06110C. I. Xyngi, M. Popov are with the Delft University of Technology, Faculty of Electrical Engineering, Mathematics and Informatics, Mekelweg 4, Delft 2628CD, The Netherlands (e-mail: IXyngi@tudelft.nl, M.Popov@tudelft.nl).

TABLE I
DG POWER RATINGS

DG Type	Snom [MVA]
SQIG 1	0.66
SQIG 2	0.66
SQIG 3	0.66
Diesel	3.125
CHP1	2.5
CHP2	2.5
μ Turbine	0.25

Detailed information concerning the dynamic models of all DG units included in the grid model can be found in [2]. A detailed description of the wind turbine dynamic models is given in [3]. A Squirrel Cage Induction Generator (SCIG) wind turbine model has been utilized, which is available in Matlab/SimPowerSystems. The diesel generator model [4] is characterized by the electrical and mechanical equations of a synchronous machine. Excitation and governor circuits of the generator are modeled as well. The model parameters of the split shaft microturbine and its detailed description can be found in [5]. Since the electromechanical behavior is of main interest for this study, the recuperator and the heat exchanger are not included in the model. Both the real power control system model and the turbine model of the microturbine are displayed in Fig. 2 and Fig. 3. The CHP model is an aggregated model consisting of 10 microturbines. All generators are connected to the distribution network through transformers. The loads are represented by constant impedances. The external system, to which the DN is connected, is assumed to behave as an ideal voltage source.

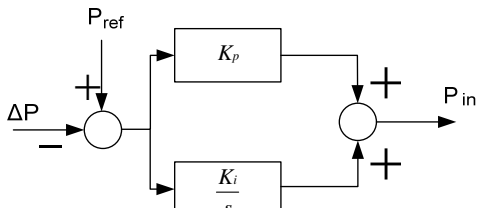


Fig. 2. Microturbine real power control system model.

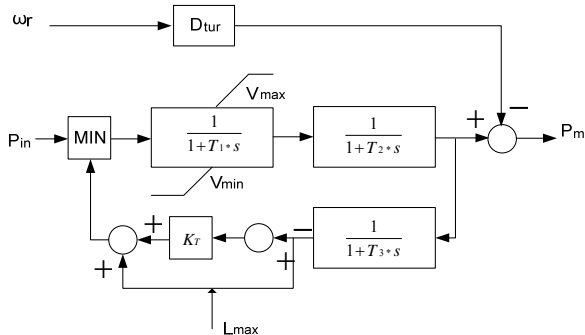


Fig. 3. Turbine model of the split shaft microturbine.

III. INVESTIGATED CASES

A. CCT Calculation

The system is subjected to various faults at different

locations. Only the worst case scenario, thus only three phase faults, have been taken into account in the investigation, since they are the most severe disturbances leading to the smallest possible CCT, although their occurrence is less probable than unbalanced single phase or phase to phase faults. In order to determine the critical clearing times, simulations are performed for different fault durations. In this study case protection of DG and network protection are disabled. First the simulation is performed for a time duration of approximately 2 s. Then the time duration is halved and new simulations are made until CCT does not converge to a solution with the precision of 1 ms. In Table II, CCT and critical generators are presented for various fault locations as shown in Fig. 1. M stands for microturbine, CHP₁ – for CHP₁ plant. For fault locations 2, 3 and 4, it turns out that all generators are stable even for a maximum fault duration of 2 s. As it can be seen from Table II, the critical system element is the microturbine, it has the smallest CCT due to its low inertia, and the critical fault location is at the high voltage side of the substation. In the worst case the CCT=509 ms. Assuming that a normal DG protection tripping time is in the order of 200 ms and the breaker opening time in the order of 100 ms, DGs transient stability is not actually endangered.

TABLE II
CRITICAL GENERATORS AND THEIR CCT

Fault Location	0	1	5	6	7	8
t_{cct} [ms]	509	514	889	584	529	620
Critical generator	M	M	CHP ₁	CHP ₁	M	M

B. Behavior of DGs During Fault Conditions and During the Post-Fault Period

Once the critical clearing times are determined, the behavior of the generators during a disturbance and following the clearance of a fault is investigated. In this particular case, the microturbine, being the most critical generator in the network, is chosen. The behavior of the microturbine following a three-phase-to-ground fault with duration of 612 ms at locations #1 and #8 is examined. One of the most meaningful observations is related to the fact that a short-circuit at the terminals of the microturbine (fault location #8) is less critical than the fault at the common busbar of the substation (fault location #1). It can be observed that even though the transient behavior of the microturbine during a short-circuit is important, in particular cases the restoration of the voltage profile in the network after the disturbance is even more critical. In this context, the post-fault voltage restoration on the common busbar is crucial. Fig. 4 shows the comparison of the variation of the substation voltage for both cases. For fault location #1 the substation voltage drops nearly to zero during the fault, then after clearance of the fault the voltage immediately rises and afterwards slowly restores to the pre-fault level. When this restoration is too slow, voltages in the

network remain to be depressed and the stability of certain generators might be lost.

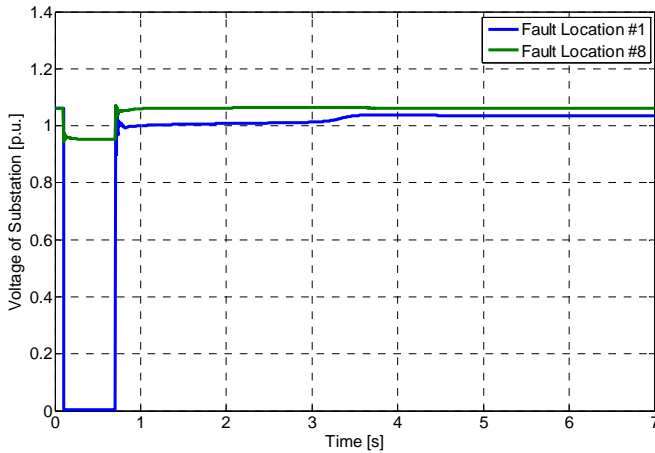


Fig. 4. Substation voltage following a three phase fault with duration of 612 ms for fault locations #1 and #8.

The variation of the microturbine terminal voltage for both cases is depicted in Fig. 5. It can be observed that although the terminal voltage during the disturbance is lower for a fault location #8 than for a fault location #1, the situation is opposite after the fault is eliminated. The justification of this observation is strongly related to the nature of the post-fault common busbar restoration. Additionally, the magnitude of the substation voltage dip plays a significant role. For the location #8, the common busbar voltage during the fault is around 0.9 p.u., while for the location #1, it is nearly 0.

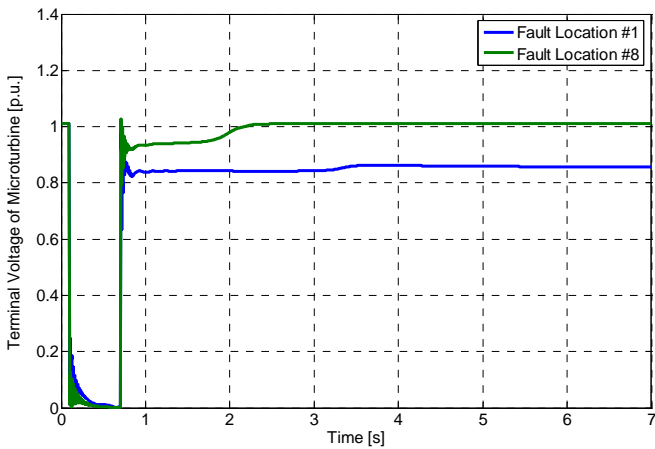


Fig. 5. Terminal voltage of microturbine following a three phase 612 ms fault for fault location #1 and #8.

Fig. 6 displays the variation of the active/reactive power and of the rotor speed of the microturbine for the different fault locations. It is shown that for the fault location #1, the microturbine cannot retain normal operation because the clearing time is greater than 514 ms. It also shows that when the fault is cleared for time spans larger than the CCT, the mechanical speed of the induction generator continues to increase. While for the same fault location the generator is delivering power during the disturbance, after the clearance of

the fault the active power of the microturbine becomes zero and no electric power is delivered to the grid. On the contrary, after the disturbance isolation of location #8, the generator retains its stability and regains its normal p.u. active power.

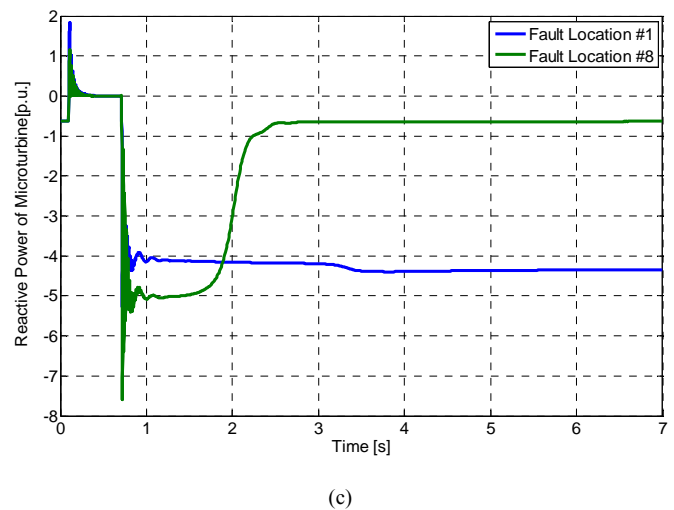
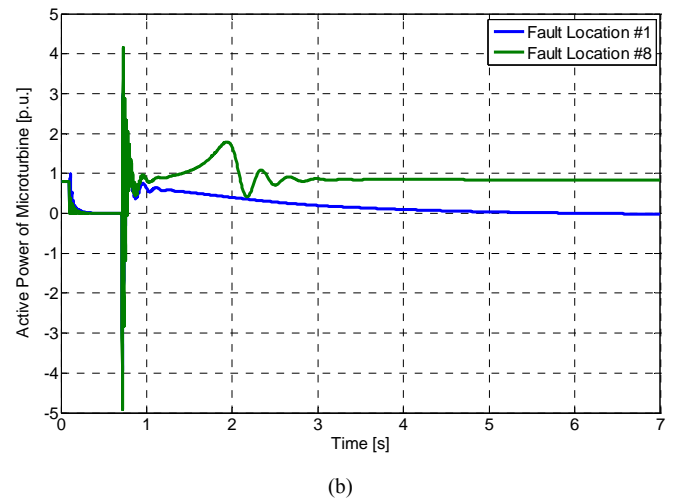
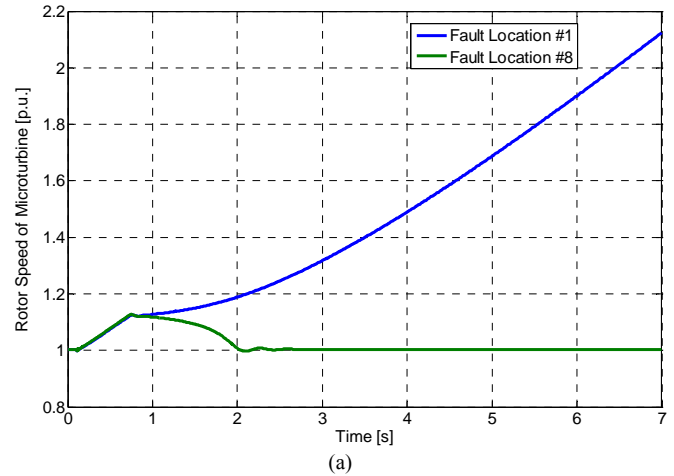


Fig. 6. (a) Rotor speed of the microturbine following a three phase fault with duration of 612 ms for fault locations #1 and #8
(b) Active power of the microturbine following a three phase fault with duration of 612 ms for fault locations #1 and #8

- (c) Reactive power of the microturbine following a three phase fault with duration of 612 ms for fault locations #1 and #8

C. CCTs Calculations for External Faults

Additionally, the CCTs of the distributed generators embedded into the investigated distribution network are determined for different external faults. The ideal voltage source of the grid model (which represents the external grid) is substituted by a three-phase programmable voltage source accompanied by its equivalent source impedance. An iterative procedure is applied for the extraction of the CCT points. The value of the voltage dip magnitude is adjusted to a certain value and the duration of the voltage dip is modified repetitively until the determination of the stability boundary (CCT). The magnitude of the voltage dip indicates the distance to the fault in the external grid. When this iteration is completed, the process starts again for a different voltage magnitude. The results are shown in Tables III, IV and V (V_{grid} is the external grid voltage) correspondingly for the microturbine, CHP1 and CHP2 units.

TABLE III
CCT OF MICROTURBINE FOR DIFFERENT EXTERNAL FAULTS

V_{grid} , p.u.	0	0.1	0.2	0.3	0.4	0.5	0.534	0.6
t_{cct} [ms]	508	535	607	718	928	1478	1979	Stable

Simulations regarding the SCIG wind turbine and diesel generator models revealed that these generators are always stable even for the worst external voltage dip depth and duration (0 p.u. and 2 s). It can be concluded that the CCTs in case of external short circuits increase with the distance to the fault. For the remaining voltage level of the external grid which is 0.6 p.u. and more there was no problem found with the transient stability.

TABLE IV
CCT OF CHP1 FOR DIFFERENT EXTERNAL FAULTS

V_{grid} , p.u.	0	0.1	0.2	0.3	0.4	0.47	0.492	0.6
t_{cct_CHP1} [ms]	554	579	674	827	1128	1641	1979	stable

TABLE V
CCT OF CHP2 FOR DIFFERENT EXTERNAL FAULTS

V_{grid} , p.u.	0	0.1	0.2	0.3	0.4	0.5	0.522	0.6
t_{cct_CHP2} [ms]	531	562	636	756	986	1622	1969	stable

IV. INVESTIGATION OF DG UNITS FAULT RIDE-THROUGH CAPABILITY

Nowadays, international standards and national grid codes

specify requirements for the connection of DG units to distribution level grids. The common practice is to immediately disconnect the units in case of a disturbance. However, as the aggregate installed capacity of DG increases, this will be no longer acceptable, and new requirements for the integration of the DG units should be proposed. Thus, it becomes important to keep them connected to the grid during and after a disturbance. In this section, the ride-through capabilities of the network embedded DG units are examined by means of their CCTs determination.

According to IEEE Std 1547 [6], the DG clearing time should be based on the during-fault voltage range. The standard states that for voltage levels less than 0.5 p.u., the recommended clearing time is 160 ms, whereas for voltage levels between 0.5 and 0.88 p.u. it is 2 s. In the Netherlands, the typical settings of the undervoltage relays of the DG are 0.8 p.u. for the voltage magnitude, and 0.2 s for the time delay [7].

The CCTs of the microturbine and the CHP unit are determined for faults at each terminal. The ride-through capabilities of the DG units are determined based on the method explained in [6]. Each equivalent model is connected through a 0.5 km cable to the programmable voltage source. The test network is implemented in Matlab / Simulink. For each applied voltage dip amplitude, the duration of the voltage dip is modified and the CCT times are determined. As expected, the results of both cases are approximately identical and are presented in Table IV.

TABLE VI
CCT OF MICROTURBINE/CHP FOR FAULTS AT ITS TERMINAL

V_{grid} , p.u.	0	0.1	0.2	0.3	0.4	0.5	0.534	0.6
t_{cct} [ms]	655	691	759	718	882	1130	1979	stable

The extracted points are utilized for the formulation of the blue curve in Fig. 7. The green CCT-voltage dip curve, (depicted in the same figure) corresponds to the points extracted in section III.C. The comparison of the two curves emphasises the fact that an external fault is worse from CCT point of view than a fault at microturbine terminals. The typical Dutch undervoltage protection settings and the undervoltage protection settings utilized by the German grid operator E.on Netz [9] (for generating units with a high symmetrical short circuit current) are also illustrated on the same figure (red and light blue curve correspondingly). A comparison between the typically used undervoltage protection settings and the derived CCT-voltage dip curves reveals that while in most cases the DGs are immediately disconnected, from stability point of view they could actually remain connected to the grid and support it after the clearance of the disturbance.

Additionally, Fig. 8 depicts the CCT-voltage dip curve of the CCT unit (blue curve). It is compared by different utilized undervoltage protection requirements at the DG interconnection point, such as Cenelec (red curve), IEEE Std.

1547-based (light blue curve) and German grid operator's Eon Netz requirements. The figure justifies the observation that the adjustment of the DG undervoltage protection settings according to the derived CCT-voltage dip curves can significantly increase the availability of the generation units. It can be also observed that national grid codes (Dutch, German) are even stricter than international standards (IEEE Std. 1547).

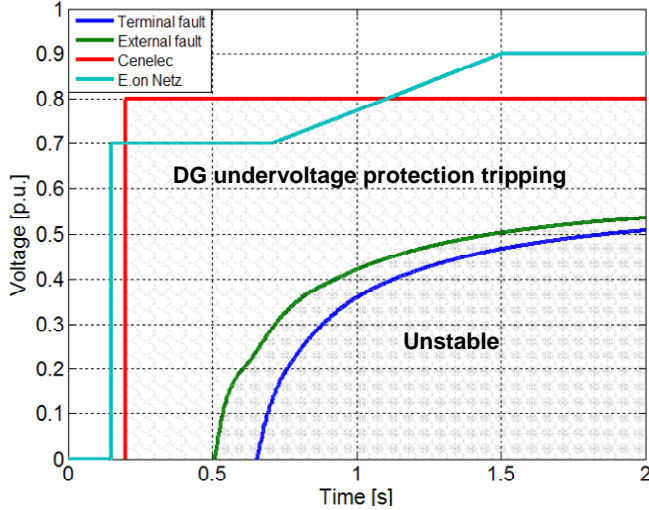


Fig. 7. CCT of the microturbine as a function of the voltage dip (remains voltage) for different external faults and for faults at its terminal. Comparison of both the typical Dutch undervoltage protection settings and the equivalent settings of the grid operator E.on Netz with the derived CCT-voltage dip curves.

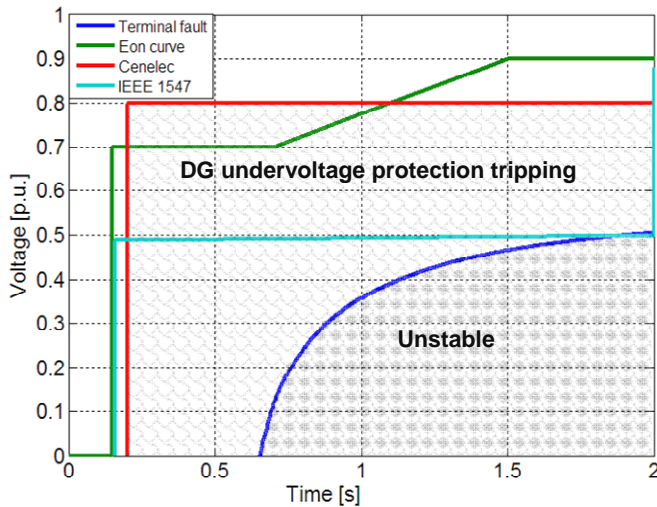


Fig. 8. CCT of the CHP unit as a function of the voltage dip (remains voltage) for faults at its terminal. Comparison of the typical Dutch undervoltage protection settings, the equivalent settings of the grid operator E.on Netz and the IEEE Std. recommended settings with the derived CCT-voltage dip curve.

The green, blue and red CCT-voltage dip traces in Fig. 9 result from points which are summarised in Tables IV, V and VI respectively. A comparison between the blue and green curve emphasises that CHP1 is less critical in terms of external faults than CHP2 from CCT point of view. The derived curves are compared with the typical Dutch

undervoltage protection settings. The frequency of DG unit disconnections can be significantly reduced when these curves are applied.

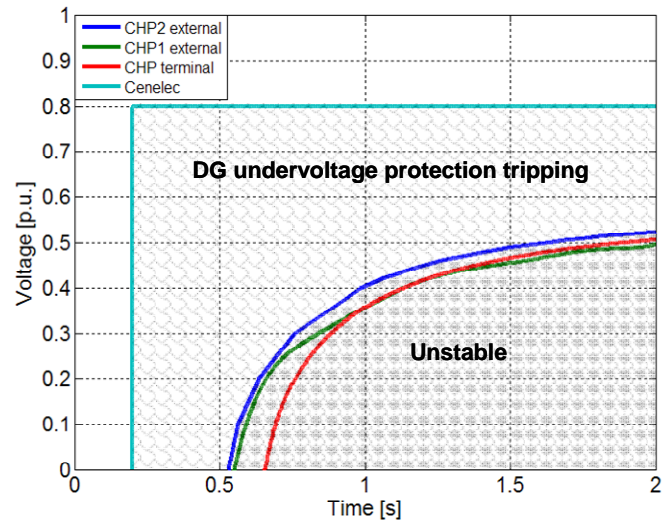


Fig. 9. CCT of the CHP1, CHP2 and CHP model as a function of the voltage dip (remains voltage) for different external faults and for faults at its terminal. Comparison of the typical Dutch undervoltage protection settings with the derived CCT-voltage dip curves.

However, a special attention has to be paid during this adjustment. The CCT curves, which are determined for a three-phase fault current applied on the terminals of the DGs do not necessarily represent the worst case situation. External faults sometimes might be more critical. Therefore to prevent instability for such situations (for the points between green and blue curves on Fig. 7) a certain safety margin has to be defined for the DG undervoltage protection settings.

Exactly the same procedure was repeated to determine the CCT curve of the rest of the DG units. The derived CHP CCT-voltage dip curve is approximately identical to the microturbine one. Simulations concerning the wind turbine and diesel generator models reveal that these generators are always stable even for the worst voltage dip magnitude and duration. Single phase to ground faults are also examined, and in this case no instabilities for the DG units were found.

V. DISCUSSION OF RESULTS

The intention of the paper is to show that normally transient stability analysis of distribution networks with DGs is required, and, if necessary, the protection settings have to be adjusted accordingly to avoid these problems. While the IEEE Std. 1547 makes no distinction between different types of DG units (it does not state directly any limits of the recommended clearing time with respect to transient stability of DG units), in the paper it is shown that each specific type of DG unit influences the transient stability and so the DG undervoltage protection settings at the interconnection point. Thus, keeping some types of DG units (for example, wind turbines) connected during a disturbance for a longer time

might result in increased support to the grid, prevent unnecessary tripping of large amount of DG units and prevent the possible power deficit in the system after fault elimination. Therefore, the authors propose that DG undervoltage protection settings should be distinguished between different types of DG units, and undervoltage settings can be determined based on transient stability analysis (also certain safety margin has to be introduced and coordination with network protection has to be performed). This is an important issue for networks with a high penetration level of DGs, like typical Dutch power systems, where the DG penetration level reaches 25-30%.

VI. CONCLUSIONS

Several studies have been carried out to determine the effect of the clearing time of a fault on the network stability of DGs. Results obtained from the studied cases are presented and discussed.

Simulations have shown that transient stability of DG units in the studied network is in general not endangered. It is also shown that for some types of DG units these problems are more evident (split-shaft microturbines), for some other types the effect is a bit less evident (CHP units, wind turbines, diesel units based on synchronous generators). Microturbine appears to be the most critical element due to its low inertia. Transient stability analysis was performed for both, microturbine and CHP units during the presence of external faults (distant faults in transmission network). Based on the analysis, it can be concluded that severe external faults are even more critical than faults on the generator terminals. External faults resulting in remaining voltage of 0.6 p.u. and higher do not endanger transient stability at all.

Present settings of DG undervoltage protection (0.8 p.u., 200 ms) might lead to massive tripping of DG units over large areas in case of fault currents at transmission voltage level. Therefore an adjustment of DG undervoltage protection is necessary to comply with fault ride-through requirements. This adjustment can be based on the CCT-voltage dip curve of the generator. By doing this, the availability of DG units can be significantly increased. However, as illustrated in this paper, some external faults might be more critical than those which occur at the generator terminals. Therefore, certain safety margin should be provided to the DG undervoltage protection settings in order to avoid possible instabilities. This conclusion is important as it permits improved optimal utilization of DG unit fault ride-through capabilities, and at the same time guarantees their transient stability.

VII. ACKNOWLEDGMENT

The research presented in this paper has been performed within the framework of the 'Intelligent Power Systems' project which is a part of the IOP-EMVT program (Innovation Oriented research Program - Electro-Magnetic Power Technology), financially supported by SenterNovem, an agency of the Dutch Ministry of Economical Affairs.

VIII. REFERENCES

- [1] IEEE Committee Report, "Proposed terms and definitions for power system stability", *IEEE Transactions on PAS-101*, pp. 1894-1898, 1982.
- [2] A. Ishchenko, "Dynamics and stability of distribution networks with dispersed generation," Ph.D. thesis, ISBN 978-90-386-1714-5, Eindhoven University of Technology, the Netherlands, 2008 (available digitally at: <http://alexandria.tue.nl/extra2/200712108.pdf>)
- [3] Matlab/Simulink Help, SimPowerSystems Blocks, Wind Turbine Induction Generator.
- [4] E. Yeager, J.R. Willis, "Modeling of Emergency Diesel Generators in an 800 Megawatt Nuclear Power Plant", *IEEE Transaction on Energy Conversion*, Vol. 8, No. 3, September 1993.
- [5] Y. Zhu, K. Tomsovic, "Development of Models for Analyzing the Load-Following Performance of Microturbines and Fuel Cells", *Elsevier Electric Power Systems Research*, No. 62, pp. 1-11, 2002.
- [6] 1547 IEEE Standard for interconnecting Distributed Resources with Electric Power Systems, IEEE, New York, USA, July, 2003.
- [7] European standard, prEN 50438, "Requirements for the connection of micro-generators in parallel with public low-voltage distribution networks", *Cenelec*.
- [8] E. Coster, A. Ishchenko, J.M.A. Myrzik, W.L. Kling, "Comparison of practical fault ride-through capability for MV-connected DG-units", *Power System Computations Conference (PSCC)*, Glasgow, Scotland, July 2008.
- [9] E.on Netz, "Grid code for high and extra high voltage", August 2003.